Archives of Materials Science and Engineering

Volume 28
Issue 3
March 2007
Pages 156-164

International Scientific Journal
published monthly as the organ of
the Committee of Materials Science
of the Polish Academy of Sciences

Structure and magnetic properties of powder HITPERM material

J. Konieczny [a], L.A. Dobrzański [a,*], J.E. Frąckowiak [b]

[a] Division of Materials Processing Technology, Management and Computer Techniques in Materials Science Institute of Engineering Materials and Biomaterials, Silesian University of Technology, ul. Konarskiego 18a, 44-100 Gliwice, Poland
[b] Institute of Material Science, University of Silesia, ul. Bankowa 12 , 40-007 Katowice, Poland
* Corresponding author: E-mail address: leszek.dobrzanski@polsl.pl

Received 15.04.2006; accepted in revised form 10.02.2007

ABSTRACT

Purpose: The aim of the work is to investigate the structure and magnetic properties of the cobalt based HITPERM amorphous alloy $Co_{68}Fe_4Mo_1Si_{13.5}B_{13.5}$ subjected high-energy ball milling and to the isothermal annealing to a combination of these two technologies.

Design/methodology/approach: The nanocrystalline ferromagnetic powders were manufactured by high-energy ball milling of metallic glasses ribbons in as state. Using the HFQS program the distributions of the magnetic hyperfine P(H) fields were determined for spectra smoothed in this way, employing the Hesse-Rübartsch method. Observations of the structure of powders were made on the OPTON DSM-940 scanning electron microscope. The diffraction examinations and examinations of thin foils were made on the JEOL JEM 200CX transmission electron microscope equipped in equipped with the EDS LINK ISIS X- ray energy dispersive spectrometer made by Oxford. Graphical analyses of the obtained X-ray diffraction patterns, as well as of the HC=f(TA) relationship were made using the MICROCAL ORIGIN 6.0 program.

Findings: The analysis of the structure and magnetic properties test results of the HITPERM powders alloy $Co_{68}Fe_4Mo_1Si_{13.5}B_{13.5}$ obtained in the high-energy ball of milling process proved that the process causes significant decrease in the magnetic properties. The magnetic properties of this material and structure and may be improved by means of a proper choice of parameters of this process as well as the final thermal treatment.

Research limitations/implications: For the soft magnetic powder material, further magnetical, composition examinations and structure are planed.

Practical implications: Feature an alternative to solid alloys are the amorphous and nanocrystalline metal powders obtained by milling of metallic glasses and make it possible to obtain the ferromagnetic nanocomposites, whose dimensions and shape can be freely formed.

Originality/value: The paper presents results of influence of parameters of the high-energy ball milling process on magnetic properties and structure of soft magnetic powder HITPERM alloy obtained in this technique. The paper compares magnetic properties and structure of the HITPERM alloy obtained in high-energy ball milling process, melt spinning technique and in a combination of these two technologies.

Keywords: Magnetic properties; Nanomaterials; Mössbauer spectrum; High energy ball milling

PROPERTIES

1. Introduction

The amorphous and nanocrystalline based on iron (FINEMET), cobalt (HITPERM) or nickel alloys obtained with the melt spinning method are characteristic of the soft magnetic properties [1-3] and best mechanical properties [4]. The materials obtained in this way are characteristic of the very high initial magnetic permeability μ, high magnetic saturation B_s, very low coercion field H_c and very low remagnetising losses. These properties may be improved by isothermal heat treatment or during heat treatment with continuously increased temperature or by heat treatment in the magnetic field [5, 6]. The nanocrystaline materials display a very low magnetic anisotropy. This is caused by the fact that the originated grains are significantly smaller from the correlation length for the ferromagnetic exchange interactions [7].

In CoSiB amorphous alloys Fe additions plays the same role as the Cu addition in the iron based amorphous alloys [8, 9]. Additions of Fe and Nb have the advantageous effect on the CoSiB alloy structure. Addition of Nb improves the thermal stability of the amorphous phase and the Fe and Nb additions make it possible to develop the nanocrystaline structure with one FeCo-A2 crystalline phase in the CoSiB amorphous alloy. The commutable Nb or Hf elements used in the 5% concentration have the equally effect on the structure [10, 11].

As the metallic amorphous and nanocrystalline materials obtained by crystallization of the metallic glasses are available in the form of thin ribbons only, the efforts are on the way to obtain the nanocrystaline powder material with various methods [12, 13].

Powders materials with amorphous and nanocrystalline structure obtained by high-energy ball milling of metallic glasses feature an alternative to solid alloys and make it possible to obtain the ferromagnetic nanocomposites, whose shape and dimensions can be freely formed [14, 15].

The goal of the work is to investigate the structure and magnetic properties of the cobalt based HITPERM $Co_{68}Fe_4Mo_1Si_{13.5}B_{13.5}$ amorphous alloy subjected to the isothermal annealing, high-energy ball milling and to a combination of these two technologies.

2. Experimental

Because of the low iron content in the examined specimens and, in addition, due to the low probability of the resonance absorption of the ^{57}Fe γ isotope radiation for the investigated materials, measurement of each Mössbauer spectrum was carried out for about one week. The resonance effect turned out to be very low in spite of the significant extension of the measurement time period and big measurement statistics. Therefore, each measured Mössbauer spectrum was smoothed, which consisted in the decomposition of the experimental spectra to the convergent Fourier series and in discarding those harmonic components that have very small input to the total dispersion, by using the Parseval relationship [16, 17]. Distributions of the magnetic hyperfine P(H) fields were determined for spectra smoothed in this way, by using the HFQS [18] program, employing the Hesse-Rübartsch method [19]. The P(H) distributions obtained are characterised by the following set of parameters:

- <H> - average value of the magnetic hyperfine field,
- <IS> - average value of the isomeric shift,
- D_H - dispersion of the P(H) hyperfine fields distribution.

The D_H parameter characterizes the hyperfine P(H) magnetic fields' distribution breadth and changes of its value are connected with fading or growth of the particular configurations of the vicinity of the 57-Fe isotope that occur in the thermal or mechanical treatment of the amorphous phase. The average values of the isomeric shift <IS> (in a smaller range) and the average values of the hyperfine magnetic field <H> are sensitive to the closest atomic neighbourhood of the 57-Fe isotope and depend on the kind of atoms surrounding the Mössbauer isotope. Analysing changes of the D_H and <H> parameters gives grounds to draw conclusions pertaining to changes occurring in the closest neighbourhood of the Mössbauer isotope, featured by ^{57}Fe.

Observations of the structure of powders were made on the Opton DSM-940 scanning electron microscope with the Oxford EDS LINK ISIS X-ray energy dispersive spectrometer at the accelerating voltage of 20 kV.

The diffraction examinations and examinations of thin foils were made on the JEOL JEM 200CX transmission electron microscope at the accelerating voltage of 200 kV equipped with the Oxford EDS LINK ISIS X-ray energy dispersive spectrometer. Thin foils were made from ribbons and powder material by cutting out disks with 3.2 mm O.D.

3. Results and discussion

The investigated $Co_{68}Fe_4Mo_1Si_{13,5}B_{13,5}$ alloy was delivered in the as quenched state and had the amorphous structure. In the electron diffraction patterns (Fig.1) the broad blurred rings are visible coming from the amorphous phase. No spot reflexes in the diffraction pattern for a test piece in the as quenched state attests to the absence of the crystalline phase in the structure. No crystalline phase was revealed in the as quenched state and the X-ray diffraction displays the evident wide-angled, diffused spectrum, characteristic for the amorphous state. The collection of all diffraction patterns obtained for the $Co_{68}Fe_4Mo_1Si_{13,5}B_{13,5}$ alloy, subjected to heat treatment in the temperature range of 400÷500°C, is presented in Figure 2.

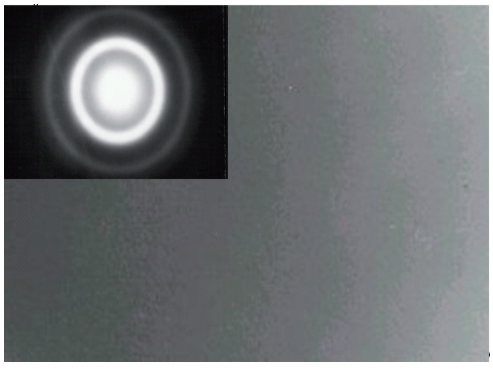

Fig. 1. Amorphous structure of the $Co_{68}Fe_4Mo_1Si_{13.5}B_{13.5}$ alloy, TEM magnification 60000x

The Mössbauer spectrum of the $Co_{68}Fe_4Mo_1Si_{13.5}B_{13.5}$ amorphous ribbon obtained in the melt spinning process is shown in Fig. 3, whereas the hyperfine fields distribution P(H) calculated for this test piece is shown in Fig. 4.

The evaluated Mössbauer spectrum is characteristic for the amorphous alloys and has a typical form of the Zeeman spectrum, consisting of 6 broadened asymmetric absorption lines. The average value of the magnetic field <H> = 21.3 T, much lower than the relevant value of the metallic iron (33.0 T), suggests that the iron atoms have atoms like Si and B in their closest neighbourhood, strongly lowering the internal magnetic field.

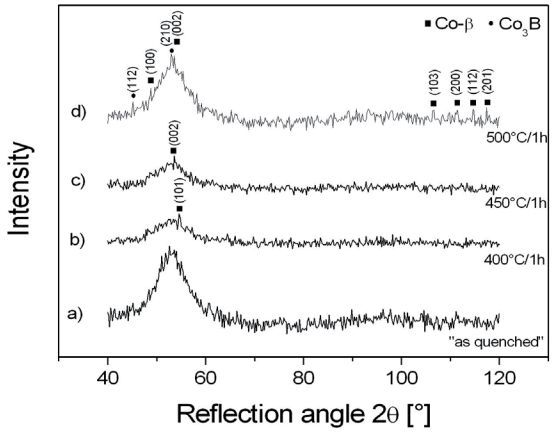

Fig. 2. X-ray diffraction pattern of the $Co_{68}Fe_4Mo_1Si_{13,5}B_{13,5}$ alloy phase analysis after annealing in the 400÷500°C temperature range

As it turns out from the research [20], the presence of Co atoms increases the value of the internal magnetic field for the Fe atoms. Therefore, the small, characteristic peak occurring in the zone of the magnetic fields of about 35.0 T may be attributed to the Fe-Co type precipitations. The big value of the proportion of lines' No (2 and 4) intensities to the (3 and 4) ones' intensities, equal to 3.65 indicates that the magnetization vector M is parallel to the test piece plane.

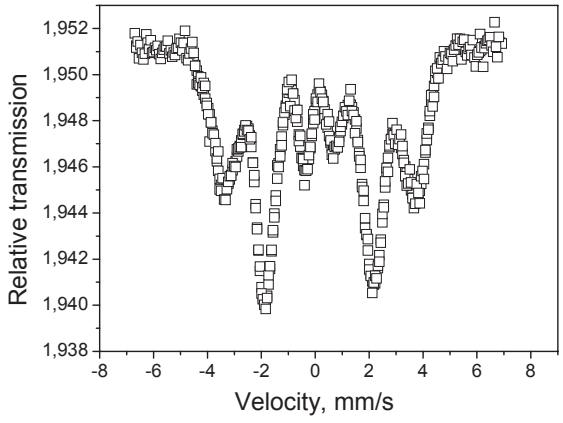

Fig. 3. The Mössbauer spectrum of the as quenched $Co_{68}Fe_4Mo_1Si_{13.5}B_{13.5}$ amorphous ribbon

It was found out in the observations carried out on the transmission electron microscope that after annealing the amorphous ribbon at temperature of 500°C, the Co-β grains increase their size and shape from spherical into the dendritic ones, dendritic grains with bigger size were also found, distributed in a rather inhomogeneous way (Fig. 5).

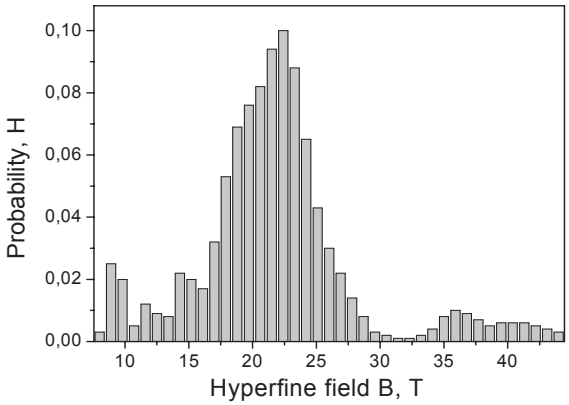

Fig. 4. Distribution of the hyperfine fields P(H) of the as quenched $Co_{68}Fe_4Mo_1Si_{13.5}B_{13.5}$ amorphous ribbon

It was found out basing on the electron diffraction that after annealing at temperature of 500°C precipitations of the crystalline phases appeared that were identified as cobalt boride (002) Co_3B and cobalt reflexes from planes (010), (002), (011) i (110) Co-β of the hexagonal with the dense arrangement of atoms.

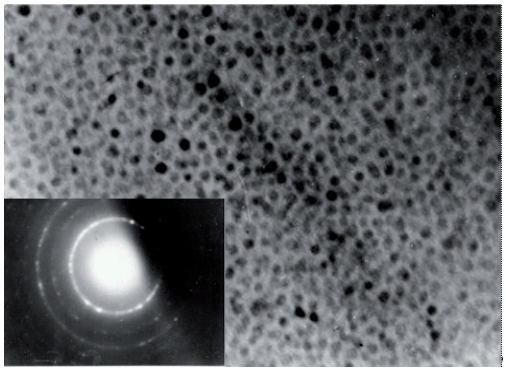

Fig. 5. Nanocrystalline structure of the $Co_{68}Fe_4Mo_1Si_{13.5}B_{13.5}$ alloy, TEM magnification 120000x

The Mössbauer spectrum annealed at the temperature of 500°C is very similar to the initial test piece's spectrum in the as quenched state. The values of the <H> and <IS> parameters, increased compared to the initial test piece indicate to increase (netto) of a number of Co atoms in the closest neighbourhood of Fe atoms in the amorphous matrix.

A significant reduction of the Fe-Co type precipitations, occurring in the initial test piece, is also visible. The changes observed are undoubtedly the result of the structural relaxation and holding of the redundant voids at an elevated temperature.

Fig. 6 shows the Mössbauer spectrum of the initial test piece annealed at 500°C and also distribution of the magnetic hyperfine P(H) fields (Fig. 7).

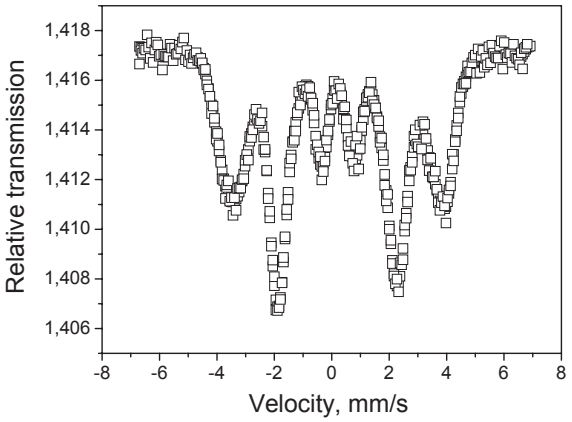

Fig. 6. The Mössbauer spectrum of the $Co_{68}Fe_4Mo_1Si_{13.5}B_{13.5}$ amorphous ribbon annealed at the temperature of 500°C

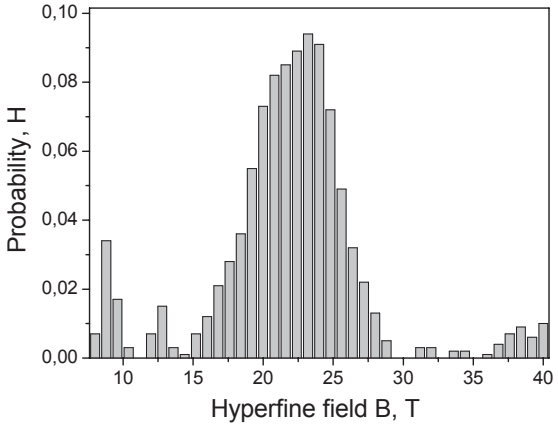

Fig. 7. Distribution of the hyperfine fields P(H) of the $Co_{68}Fe_4Mo_1Si_{13.5}B_{13.5}$ amorphous ribbon annealed at the temperature of 500°C

The powders obtained have the highest portion of the 400÷800 μm fraction (Fig. 8) at the beginning stage of milling of the $Co_{68}Fe_4Mo_1Si_{13,5}B_{13,5}$ amorphous alloy. The most probable sizes in the powder grains population (mode) are 719 μm for the material obtained after 4 hours of milling, 476 μm after 5 hours, 95 μm after 10 hours, and 12 μm after 15 hours.

Milling the material for 20 hours causes further size reduction of particles (Fig. 9). The highest portion of ≈ 15% was found out for particles from the range of 13÷18 μm, the arithmetic average of the powders diameter is 14.88 μm.

Powder obtained after 40 hours of milling process is characteristic for its bimodal size distribution (Fig. 10). The highest portion of ≈ 7% was found out for particles from ranges of 31÷40 μm and 450÷500 μm, and the arithmetic average diameter of powders is 22.63 μm.

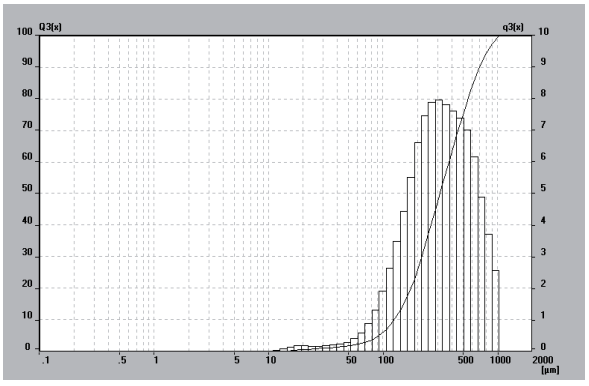

Fig. 8. The cumulative percentage portions curve and the grain size distribution curve for the powder obtained after 5 hours long milling of the $Co_{68}Fe_4Mo_1Si_{13,5}B_{13,5}$ amorphous ribbon of the metallic glass

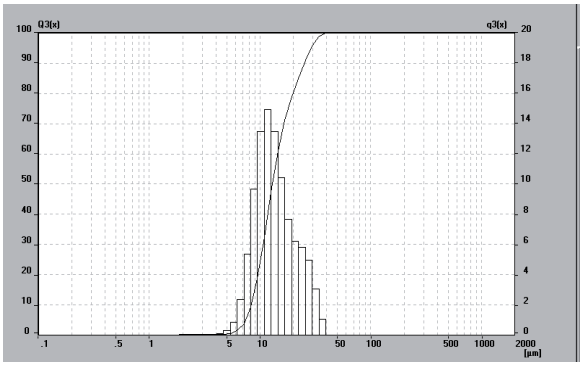

Fig. 9. The cumulative percentage portions curve and the grain size distribution curve for the powder obtained after 20 hours long milling of the $Co_{68}Fe_4Mo_1Si_{13,5}B_{13,5}$ amorphous ribbon of the metallic glass

Extending the milling time to 80 hours leads to the essential increase of the percentage portion of minute particles 0.1÷5 μm and the arithmetic average of the entire population is 172 μm.

It turns out from the cumulative percentage portions curves and from the powder grain size distribution curves that the most significant break-up of the material takes place at the initial milling stage, i.e., up to 25 hours.

Powder grains obtained by milling of the $Co_{68}Fe_4Mo_1Si_{13,5}B_{13,5}$ amorphous ribbon are flake-shaped after milling for 5 hours with the dominating longitudinal dimension (Fig. 11). Powder grains obtained after milling for 10 hours get smaller, yet flake-shaped grains still occur and smaller grains appear with the nearly spherical shape.

The spherical shape dominates among powder grains obtained after 15 hours long milling; however, the flake-shaped grains were observed also with big magnifications (Fig. 11). Spherical grains dominate in the powder obtained after 25 hours of milling with a small number of flake-shaped grains. Powder grains obtained after 60 hours of milling are characteristic for their spherical shape with no sharp edges (Fig. 12).

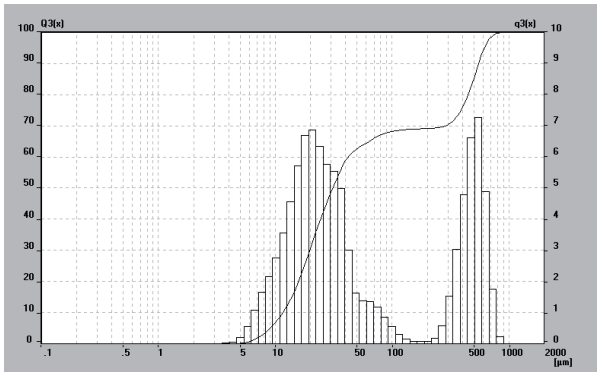

Fig. 10. The cumulative percentage portions curve and the grain size distribution curve for the powder obtained after 40 hours long milling of the $Co_{68}Fe_4Mo_1Si_{13,5}B_{13,5}$ amorphous ribbon of the metallic glass

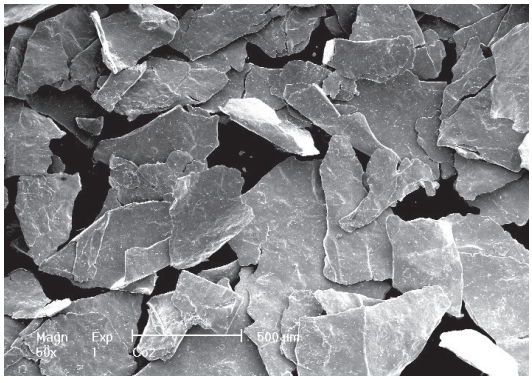

Fig. 11. Image of powder grains obtained from the $Co_{68}Fe_4Mo_1Si_{13,5}B_{13,5}$ amorphous ribbon subjected to the high energy milling for 5 hours, electron scanning microscope

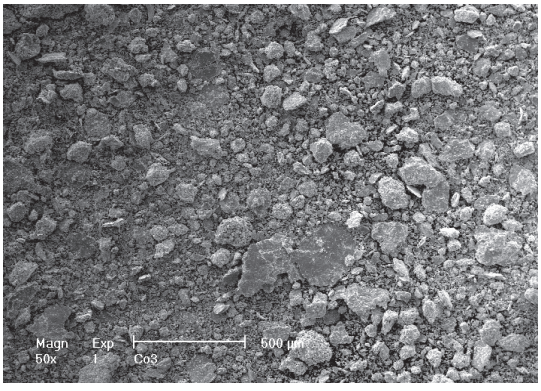

Fig. 12. Image of powder grains obtained from the $Co_{68}Fe_4Mo_1Si_{13,5}B_{13,5}$ amorphous ribbon subjected to the high energy milling for 15 hours, electron scanning microscope

Basing on the X-ray phase analysis carried out of the powders obtained from the $Co_{68}Fe_4Mo_1Si_{13,5}B_{13,5}$ amorphous ribbon in the high energy milling process after 10, 40, and 80 hours of milling, the wide-angle peaks were revealed in the angle range of $2\theta=45\div60°$, with the high intensity caused by the amorphous phase, and – most probably – by the Co-β phase from the (101) plane.

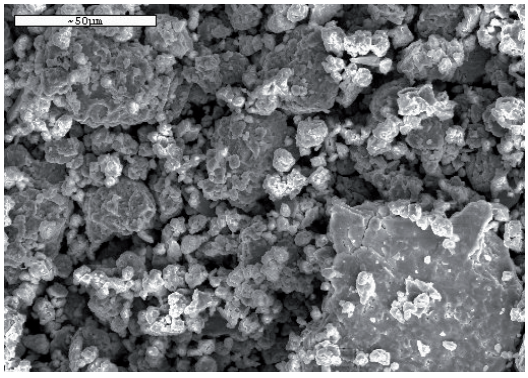

Fig. 13. Image of powder grains obtained from the $Co_{68}Fe_4Mo_1Si_{13,5}B_{13,5}$ amorphous ribbon subjected to the high energy milling for 60 hours, electron scanning microscope

Fig. 14 presents the Mössbauer spectrum evaluated for the powder test piece obtained from the input amorphous ribbon after 15 hours of milling; whereas Fig. 15 shows the relevant distribution of the P(H) hyperfine fields.

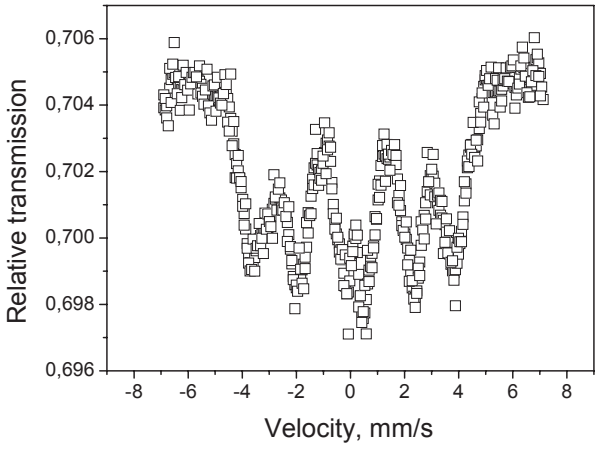

Fig. 14. The Mössbauer spectrum of the powder obtained from the $Co_{68}Fe_4Mo_1Si_{13.5}B_{13.5}$ amorphous ribbon after 15 hours of milling

The Mössbauer spectrum of this test piece has the worst quality, which may result from its iron depletion due to the milling process. Anyway, analysis of the smoothed spectrum indicates that a clear separation of magnetic properties occurs in the test piece, connected perhaps with the specific distribution of the nanocrystalline grains with the diametrically different diameters. Two peaks are visible on the P(H) curve, one of which refers to the field value of H1=13.0 T, whereas the second one to the field value of H2=22.0 T. The H_2 field value is close to the average field value for the amorphous test piece annealed at the temperature of 500°C. However, the small value of the field value H_1, may be connected with grains of very small

diameters, for which portion of the low-iron configurations of neighbourhoods connected with grain surfaces may be significant. It cannot also be ruled out that the abovementioned grains have superparamagnetic properties.

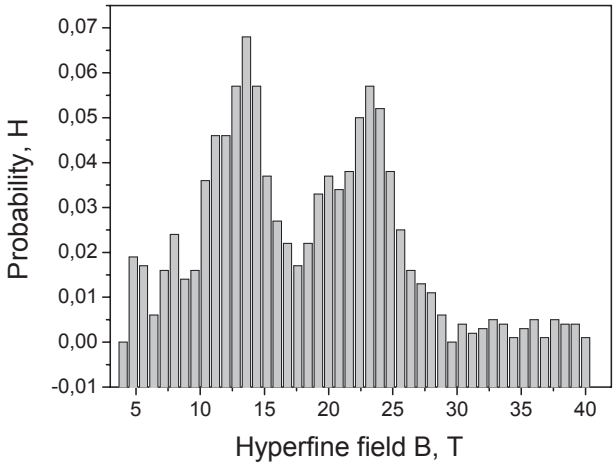

Fig. 15. Distribution of the hyperfine fields P(H) of the powder obtained from the $Co_{68}Fe_4Mo_1Si_{13.5}B_{13.5}$ amorphous ribbon after 15 hours of milling

Fig. 16 presents the evaluated Mössbauer spectrum of a powder test piece obtained from the input ribbon after 20 hours of milling; whereas, Figure 17 presents the relevant distribution of the magnetic hyperfine fields P(H).

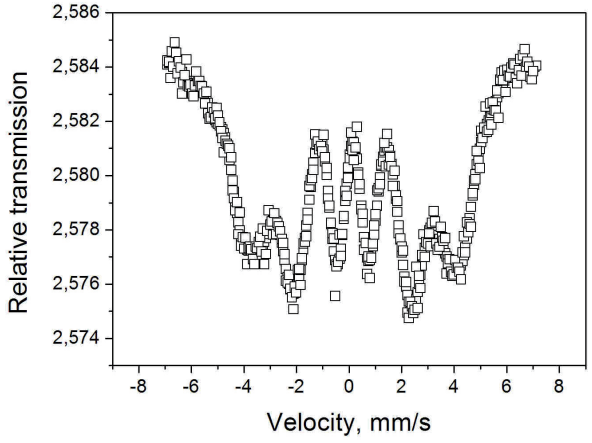

Fig. 16. The Mössbauer spectrum of the powder obtained from the $Co_{68}Fe_4Mo_1Si_{13.5}B_{13.5}$ amorphous ribbon after 20 hours of milling

The shape of the Mössbauer spectrum shows, that the material under investigation consists in amorphous grain. The P(H) hyperfine fields distribution is wide and symmetrical, what testifies about steady grain participation with different diameter.

Observations on the transmission electron microscope (TEM) revealed that the high energy milling carried out even for a relatively short time of 25 hours results in development of the nanocrystalline structure (Fig. 18). This structure differs from the nanostructure obtained by the isothermal annealing of amorphous ribbons, it is more irregular, inhomogeneous, and grains present in it are very diversified as regards their shape and size. Basing on analysis of the diffraction patterns from the transmission electron microscope phases of Co-β, Co_2B cobalt boron, Co_2Si and $CoSi_2$ cobalt silicides, as well as the Fe_2B phase were revealed in structure of powder obtained after 25 hours of milling.

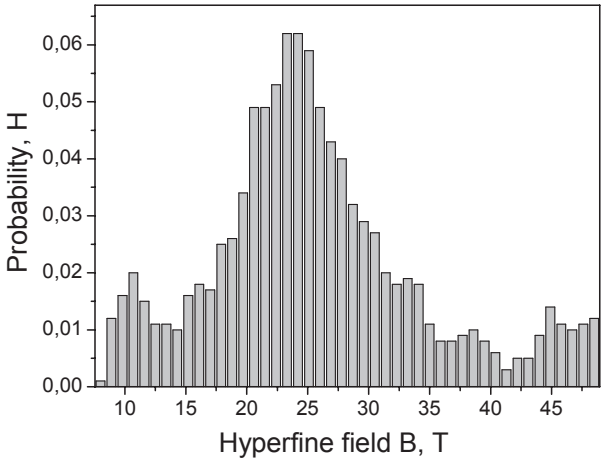

Fig. 17. Distribution of the hyperfine fields P(H) of the powder obtained from the $Co_{68}Fe_4Mo_1Si_{13.5}B_{13.5}$ amorphous ribbon after 15 hours of milling

Fig. 19 presents the evaluated Mössbauer spectrum of a powder test piece obtained from the input ribbon after 25 hours of milling; whereas, Figure 20 presents the relevant distribution of the magnetic hyperfine fields P(H).

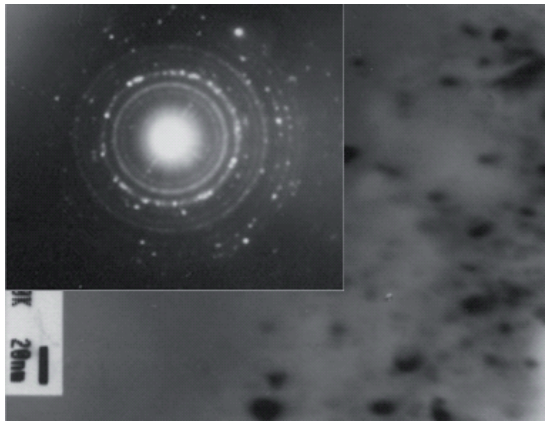

Fig. 18. Structure of powder grain obtained after 25 hours of high energy milling of the $Co_{68}Fe_4Mo_1Si_{13,5}B_{13,5}$ amorphous ribbon and diffraction pattern of the powder grain; TEM

The Mössbauer spectrum of this test piece is characteristic also for the amorphous material. The field distribution P(H) is

shifted towards the lower values of the magnetic fields, compared to the previous test piece. This effect is surely connected with extending the milling time and the resulting decrease of the grains diameter. One should note small peaks appearing in the P(H) distribution for the magnetic fields range bigger than 30.0 T, connected with grains enriched with Fe and Co.

The nanocrystaline structure was revealed in the powder material obtained by grinding the $Co_{68}Fe_4Mo_1Si_{13,5}B_{13,5}$ ribbon annealed before for 1 hour at the temperature of 500°C. The following phases were identified in the analysis of diffraction patterns obtained on the transmission microscope: Co-α, Co-β, $CoSi_2$, and Fe_2B.

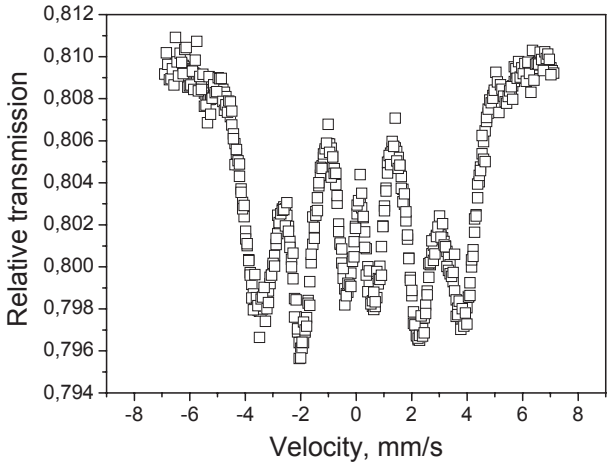

Fig. 19. The Mössbauer spectrum of the powder obtained from the $Co_{68}Fe_4Mo_1Si_{13.5}B_{13.5}$ amorphous ribbon after 25 hours of milling

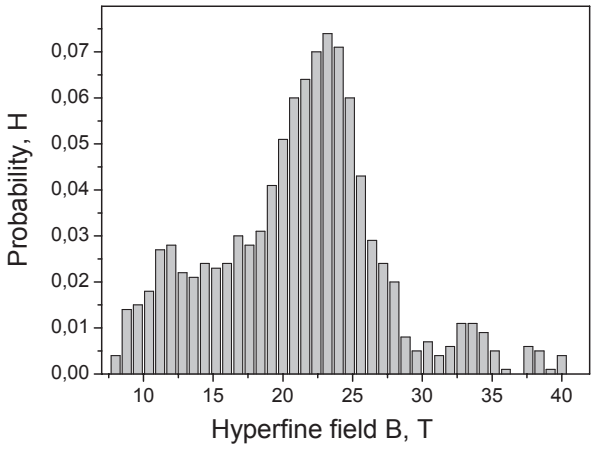

Fig. 20. Distribution of the hyperfine fields P(H) of the powder obtained from the $Co_{68}Fe_4Mo_1Si_{13.5}B_{13.5}$ amorphous ribbon after 25 hours of milling

Fig. 21 presents the Mössbauer spectrum evaluated for the powder test piece obtained from the input ribbon annealed at the temperature of 500°C and milled for 2 hours; whereas Fig. 22 shows the relevant distribution of the P(H) hyperfine fields.

The Mössbauer spectrum of this test piece has the evident discrete constituent lines, connected with the phase of the low magnetic field. Admittedly, the separation of peaks is not that clearly visible on the P(H) distribution, as it is in case for the test piece milled for 15 hours; however, this reasoning seems to be correct also in this case.

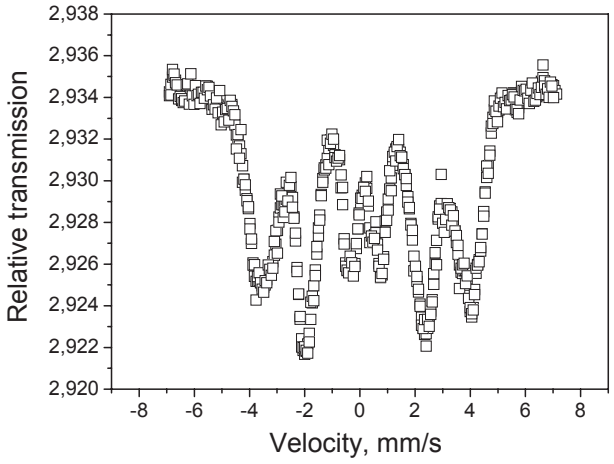

Fig. 21. The Mössbauer spectrum of the powder obtained from the $Co_{68}Fe_4Mo_1Si_{13.5}B_{13.5}$ amorphous ribbon annealed at the temperature of 500˚C after 2 hours of milling

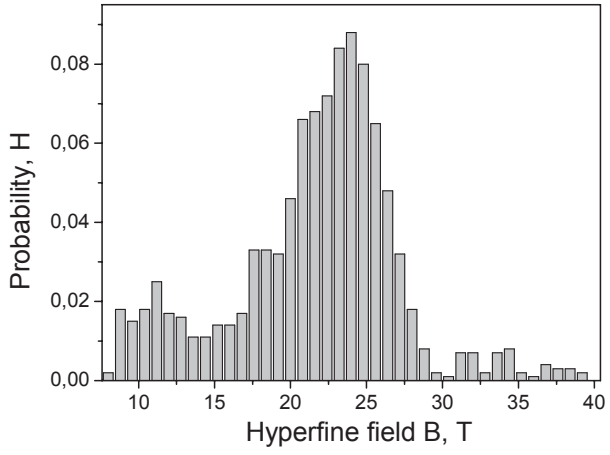

Fig. 22. Distribution of the hyperfine fields P(H) of the powder obtained from the $Co_{68}Fe_4Mo_1Si_{13.5}B_{13.5}$ amorphous ribbon annealed at the temperature of 500˚C after 2 hours of milling

4. Conclusions

The analysis of the magnetic properties test results of the of the $Co_{68}Fe_4Mo_1Si_{13.5}B_{13.5}$ powders obtained in the high-energy ball of milling process proved that the process causes significant decrease in the magnetic properties.

It was found out in observations on the scanning electron microscope that along with the milling time increase the powder particles size decreases, and that their shape changes also during the process. The powder grains were flake-sized at the first stage of the process, and actually they were parts of the ribbons. However, as the milling time grows the grains become spherical with a clear tendency to get smaller. Decreasing of the powder particles size is very intensive during the first hours of milling; whereas, at the later stage of the process changes of the average particle size are of the order of several percent per milling hour. The acquired results are comparable to results obtained by other authors [21, 22].

Basing on magnetic properties tests of the powder material, it was found out that compared to the magnetic properties of the amorphous ribbons as their precursor, the high energy milling process deteriorates their magnetically soft properties.

The powder material obtained in the high energy milling process, subjected to the isothermal annealing at the optimum temperature, which is determined by the milling time period

Results of analysis made using the Mössbauer spectroscopy confirm that in the $Co_{68}Fe_4Mo_1Si_{13,5}B_{13,5}$ alloy, in the obtained powder material a clear separation occurs of magnetic properties, connected most probably with the specific distribution of the nanocrystalline grains with the diametrically different diameters. One cannot either rule out that powder grains with the very small diameter have the superparamagnetic properties.

On the basis of the research done, it was stated that the process of the high-energy ball milling combined with thermal crystallisation of the $Co_{68}Fe_4Mo_1Si_{13.5}B_{13.5}$ alloy, results in the production of the nanocrystalline powder material. The structure and magnetic properties of this material may be improved by means of a proper choice of parameters of this process as well as the final thermal treatment.

Additional information

The presentation connected with the subject matter of the paper was presented by the authors during the 14th International Scientific Conference on Achievements in Mechanical and Materials Engineering AMME'2006 in Gliwice-Wisła, Poland on 4th-8th June 2006

References

[1] Y. Yoshizawa, S. Fujii, Microstructure and magnetic properties of FeCoMoBC alloys, Journal of Magnetism and Magnetic Materials 290–291 (2005) 1543–1546.

[2] S. Lesz, R. Nowosielski, B. Kostrubiec, Z. Stokłosa, Crystallization kinetics and magnetic properties of a Co-based amorphous alloy, Journal of Achievements in Materials and Manufacturing Engineering 16 (2006) 35-39.

[3] J. Konieczny, L. A. Dobrzański, J.E. Frąckowiak, Structure and properties of the powder obtained from the amorphous ribbon, Journal of Achievements in Materials and Manufacturing Engineering 18 (2006) 143-147.

[4] D. Szewieczek, S. Lesz, Influence of structure on the evolution of magnetic and mechanical properties of amorphous and nanocrystalline $Fe_{85.4}Hf_{1.4}B_{13.2}$ alloy, Proceedings of the 13th International Scientific Conference „Achievements in Mechanical and Materials Engineering" AMME'2005, Gliwice-Wisła, 2005, 637-640.

[5] Y. Yoshizawa, Magnetic properties and applications of nanostructured soft magnetic materials, Scripta Materialia 44 (2001) 1321-1338.

[6] D. Szewieczek, T. Raszka, Structure and magnetic properties of $Fe_{63.5}Co_{10}Cu_1Nb_3Si_{13.5}B_9$ alloy, Journal of Achievements in Materials and Manufacturing Engineering 18 (2006) 179-182.

[7] A. Gehrmann, Nickel–iron alloys with special soft magnetic properties for specific applications, Journal of Magnetism and Magnetic Materials 290–291 (2005) 1419–1422.

[8] A. Serebryakov, V. Sedykh, N. Novokhatskaya, V. Stelmukh, Mössbauer study of primary crystallization in amorpfous $(Co_{77}Si_{13,5}B_{9,5})_{93}Fe_4Nb_3$, NanoStructured Materials 7 (1996) 461-464.

[9] A. Serebryakov, L. Voropaeva, Yu. Levin, N. Novokhatskaya, G. Abrosimova, Nanocrystallization of amorphous Co-Si-B alloys: effect of Fe+Nb additions, NanoStructured Materials 4 (1994) 851-854.

[10] V. Stelmukh , A. Gurov, L. Voropaeva, N. Novokhatskaya, A. Serebryakov, Nanocrystallization of amorphous Co-Si-B alloys with strong compound forming additions, Journal of Non-Crystalline Solids 192 and 193 (1995) 570-573.

[11] S.S. Sikder, M.A. Asgar, The kinetics of atomic and magnetic ordering of Co-based amorphous ribbons as affected by iron substitution, Termohimica Acta 326 (1999) 119-122.

[12] L.A. Dobrzański, R. Nowosielski, J. Konieczny, The structure and magnetic properties of magnetically soft cobalt base nanocrystalline powders and nanocomposites with silicon binding, Journal of Materials Processing Technology 155-156 (2004) 1943-1949.

[13] P. Nandi, P.P. Chattopadhyay, P.M.G. Nambissan, F. Banhart, H.J. Fecht, I. Manna, Microstructural aspects and positron annihilation study on solid, state synthesis of amorphous and nanocrystalline $Al_{60-x}Ti_{40}Si_x$, alloys prepared by mechanical alloying, Journal of Non-Crystalline Solids 351 (2005) 2485-2492.

[14] J. Jakubowicz, J.-M. Le Breton, Structure and magnetic properties of, $(Nd,Dy)_{16}(Fe,Co)_{76-x}Ti_xB_8$ powders prepared by mechanical alloying, Journal of Magnetism and Magnetic Materials 301 (2006) 279-286.

[15] P. Gramatyka, A. Kolano-Burian, R. Kolano, M. Polak, Nanocrystalline iron based powder cores for high frequency applications, Journal of Achievements in Materials and Manufacturing Engineering 16 (2006) 99-102.

[16] G.M. Jenkins, D.G. Watts, Spectral Analysis and its Applications, HOLDEN-DAY, Cambridge, 1969.

[17] S. Chakraborty, M.C. Parker, R.J. Mears, A Fourier (k-) space design approach for controllable photonic, band and localization states in aperiodic lattices, Photonics and Nanostructures – Fundamentals and Applications 3 (2005) 139-144.

[18] Z. Bojarski, J. Frackowiak, Proceedings of the Conference On Applied Crystallization, Spectra smoothed of the Mössbauer spectrum by using the HFQS, Cieszyn, Ed. Z. Bojarski, J. Paduch, H. Krztoń, (1990) 114-119.
[19] J. Hesse, A.J. Rubartsch, Model independent evaluation of overlapped Mössbauer spectra, Journal of Physics E (1974) 526-531.
[20] Beak-Hee Lee, Bong Su Ahn, Dae-Gun Kim, Sung-Tag Oh, Hyeongtag Jeon, Jinho Ahn, Young Do Kim, Microstructure and magnetic properties of nanosized Fe–Co alloy powders synthesized by mechanochemical and mechanical alloying process, Materials Letters 57 (2003) 1103-1107.
[21] H.R. Madaah Hosseini, A. Bahrami, Preparation of nanocrystalline Fe–Si–Ni soft magnetic powders by mechanical alloying, Materials Science and Engineering B 123 (2005) 74-79.
[22] H. Moumeni, S. Alleg, J.M. Greneche, Structural properties of $Fe_{50}Co_{50}$ nanostructured powder prepared by mechanical alloying, Journal of Alloys and Compounds 386 (2005) 12-19.